Electronic Supplementary Information (ESI) for Chemical Communications. This journal is (c) The Royal Society of Chemistry 2023.

Electronic Supplementary Information (ESI)

A nanowire-on-microrod polyaniline@FeS_2 hybrid as cathode in high-performance Al-ion batteries

Haiyuan Bai[a], Jing Xu[a], Jinyun Liu[a], Tianli Han*[,a], Junjie Niu*[,b]

Experimental section

Preparation of MIL-88A: Firstly, 0.518 g of fumaric acid (AR, 99.5%, Aladdin) was added to 75 mL of deionized water and stirred (DF-101S, LICHEN, 1000r/min) in a water bath (DF-101S, LICHEN) at 70 °C for 15 min to form the solution A. Subsequently, 1.192 g of $Fe(NO_3)_3 \cdot 9H_2O$ (AR, 98.5%, Macklin) was dissolved in 13 mL deionized water to form the solution B. Then the solution B was mixed with solution A under stirring in a 70 °C water bath for 30 min. Then the mixture was added into a Teflon liner (50 mL, BK) in an autoclave (JINGHONG, 135 L) at 110 °C for 6 h. The collected precipitate was centrifuged (TG16G, 7000r/min) with deionized water and ethanol for 3 times. Finally the obtained sample was dried 12 h at 70 °C (JINGHONG, 135 L).

Preparation of FeS_2 microrods: 3.0 g of sulfur powder (AR, 99.5%, Aladdin) was placed in a ceramic boat that was located at the upstream of a tube furnace (OTF-1200X, HF-Kejing). In parallel, 0.15 g of as-prepared MIL-88A was placed in the downstream. Before heating, the furnace was pumped by a rotary vacuum pump (VALUE, FY-1C-N) to reach a pressure of 2.0 Pa with oxygen less than 0.01 ppm. Then the furnace was heated to 450 °C for 1.0 h under Ar (XC-Liyuan, 99.999%). After the furnace was cooled down to room temperature, the sample was collected.

Preparation of the PANI@FeS_2 hybrid: The PANI nanowires were coated on the as-prepared FeS_2 microrods in an ice bath (DF-101S, LICHEN). In a typical experiment, 0.1 g of FeS_2 microrods was dispersed in a 60 mL solution with 0.5 mol L^{-1} H_2SO_4 under stirring (DF-101S, LICHEN) at –5 °C. Then 0.355 mL of aniline (AR, 99.5%, Aladdin) was added. In parallel, 0.568 g of ammonium persulfate (AR, 98%, Aladdin) was added to a 40 mL solution with 0.5 mol L^{-1} H_2SO_4, which was mixed with the FeS_2 microrods solution. After magnetically stirring (DF-101S, LICHEN) for 10 h, the sample was centrifuged and rinsed by deionized water and ethanol for 3 times. After drying at 70 °C overnight, the PANI@FeS_2 hybrid was prepared for battery assembly.

Characterizations: Crystal structure of the sample was analyzed by X-ray diffractometer (XRD SMART APEX II Brook, Cu Kα X-ray wavelength=1.5418 Å). Scanning electron microscope (SEM, Hitachi 8100, 5 KV) and transmission electron microscope (TEM, Hitachi HT-7700, 120 KV) were applied to check the sample morphology. The lattice fringes of the sample were obtained by using high-resolution TEM (HRTEM, TecnaiG220S-Twin, 200 KV). The chemical composition of the sample was verified by using energy dispersive X-ray spectroscopy (EDX, Hitachi 8100, 15 KV). The bonding energy of the sample was checked by using X-ray photoelectron spectroscopy (XPS, EscalAB250, Al Kα hν=1486.6 eV). The functional groups of the sample were checked by Fourier Transform infrared spectroscopy (FTIR-21, SHIMADZU). The BET surface area of the sample was measured by nitrogen at 77 K by ASAP Micromeritics Tristar 2460 instrument. Thermogravimetric analysis (TGA) was performed under N_2 on a thermogravimetric analyzer (NETZSCH, STA-2500).

Electrochemical property and battery tests: First, 70 wt% PANI@FeS_2 hybrid and 20 wt% conductive carbon black were mixed for 30 min, then 10 wt% polyvinylidene fluoride was added as a binder. Subsequently, a slurry was formed by adding 0.5 mL of N-methylpyrrolidone (NMP, 99.99%). Then the slurry was stirred under 1200 r/min by an agitator (MYP13-2, CHIJIU). After stirring for 8 h, the slurry was coated on a carbon paper via drop casting with a thickness of about 200 μm. Then the sample was dried in a vacuum oven (JINGHONG, 70 L) at 80 °C for 24 h. The dried sample was cut into a circular disc with a diameter of 12 mm, which

was used as cathode electrode. A molybdenum sheet (QingYuan, 99.99%, 0.02 mm) with a diameter of 20 mm and a thickness of 0.02 μm was used to prevent the cell from electrolyte corrosion. A pure aluminum sheet (QiRui, 99.99%, 0.5 mm) was used as anode electrode. A glass fiber membrane (Whatman, GF/D, 0.5 mm) was used as separator. $AlCl_3$ in [EMIm]Cl (DoDoChem) with a molar ratio of 1.3:1 was used as ionic electrolyte. A CR-2032 coin cell was assembled inside an Ar-filled glove box (MIKROUNA, Super1220/750/900) with less than 0.01 ppm of moisture and oxygen. The electrochemical property was checked after resting for 12 h. The battery cycling performance was tested on a battery tester (NEWARE) in the potential range of 0.01-1.9 V. Reaction resistance was investigated by using galvanostatic intermittent titration technique (GITT, NEWARE). Cyclic voltammetry (CV) was tested by an electrochemical workstation (CHI660e, 0.01-1.9 V).

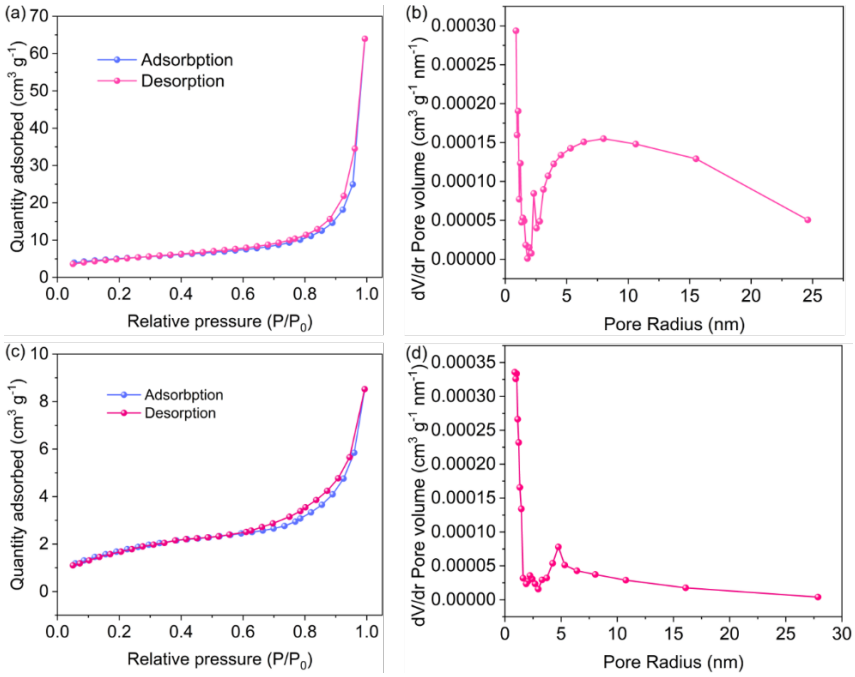

Fig. S1. (a) N_2 adsorption-desorption isotherms and (b) pore-size distribution of the PANI@FeS_2 hybrid. (c) N_2 adsorption-desorption isotherms and (b) pore-size distribution of the pure FeS_2.

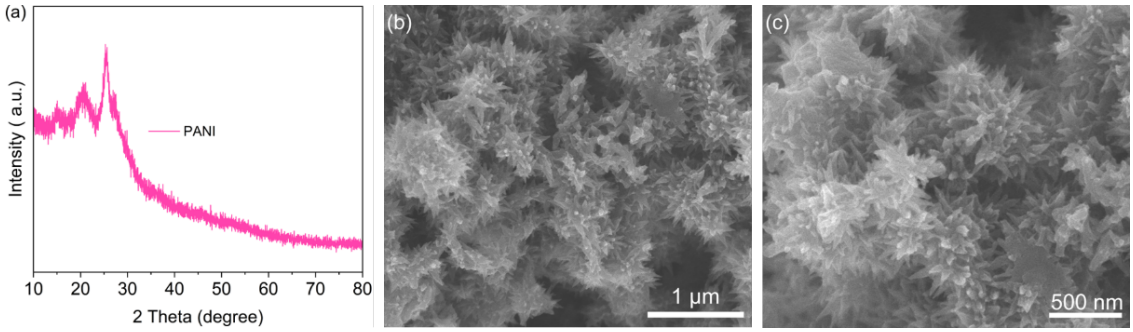

Fig. S2. (a) XRD pattern and (b,c) SEM images of pure PANI.

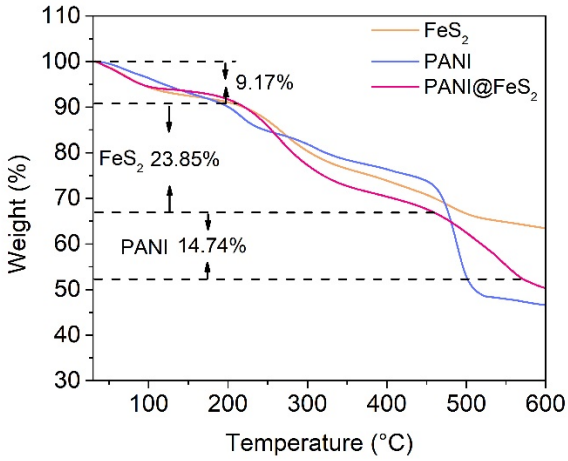

Fig. S3. TGA curves of FeS_2, PANI and PANI@FeS_2 hybrid.

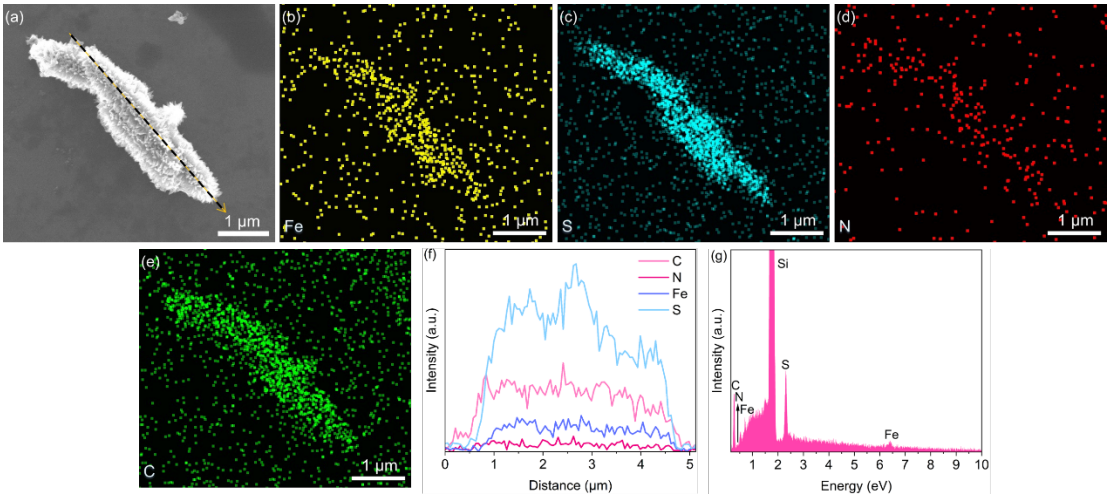

Fig. S4. (a) SEM morphology and (b-e) the corresponding elemental mappings of the as-obtained PANI@FeS_2 hybrid. (f) Line-scanning and (g) EDS spectrum of the PANI@FeS_2.

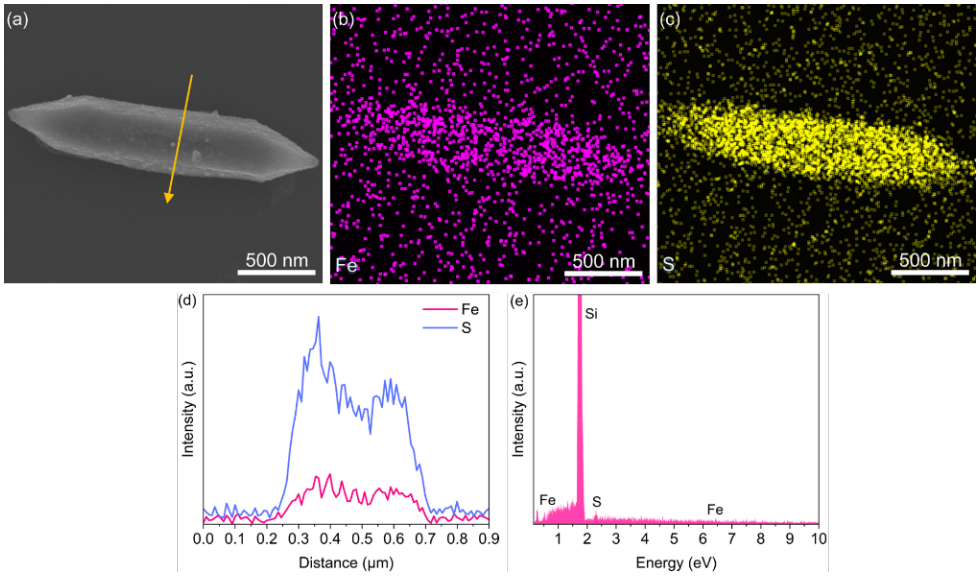

Fig. S5. (a) SEM morphology, (b,c) the corresponding elemental mappings, (d) line-scanning, and (e) EDS spectrum of pure FeS_2 microrod.

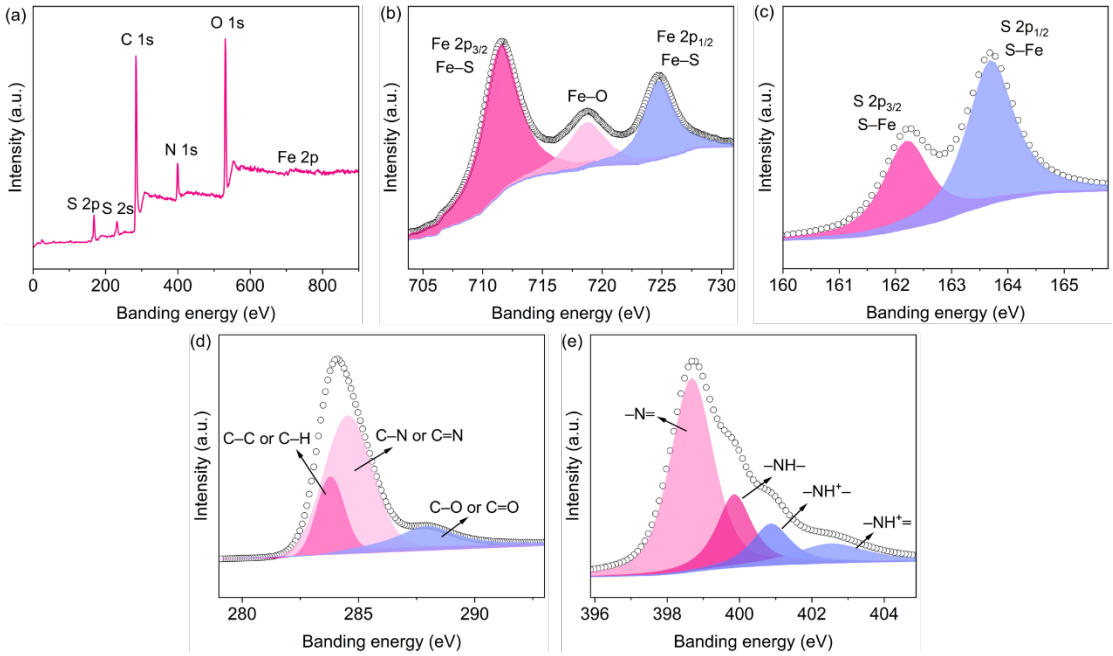

Fig. S6. (a) Full spectrum survey, (b) Fe 2p, (c) S 2p, (d) C 1s, and (e) N 1s XPS spectra of the PANI@FeS_2.

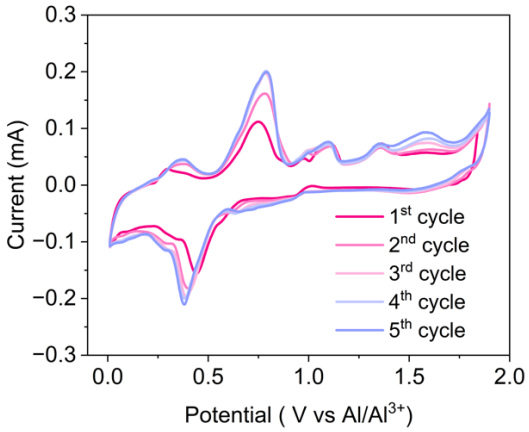

Fig. S7. CV curves of pure FeS_2 microrods. The scanning rate was 0.1 mV s^{-1}.

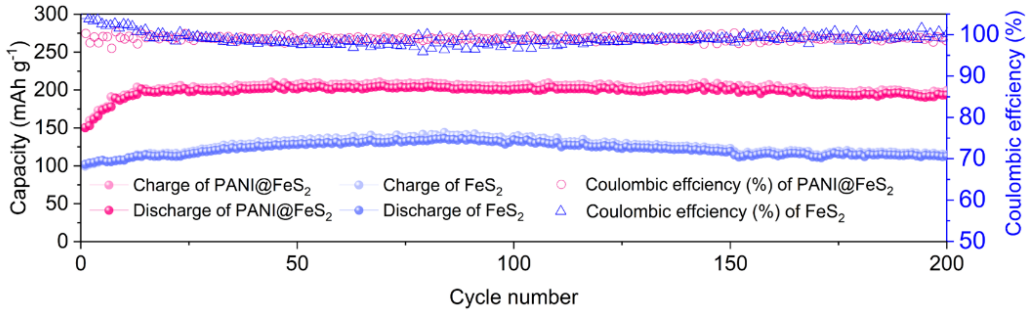

Fig. S8. Cycling performance of PANI@FeS_2 hybrid and pure FeS_2 microrods at 1.0 A g^{-1}.

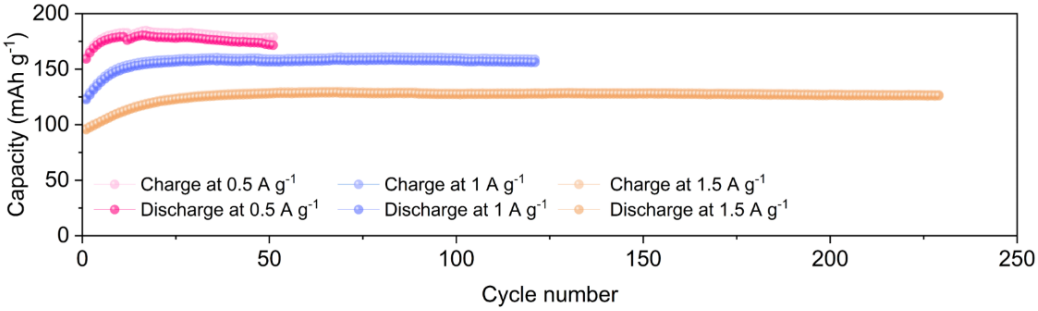

Fig. S9. Cycling performance of the battery with PANI as cathode at 0.5, 1, and 1.5 A g^{-1}.

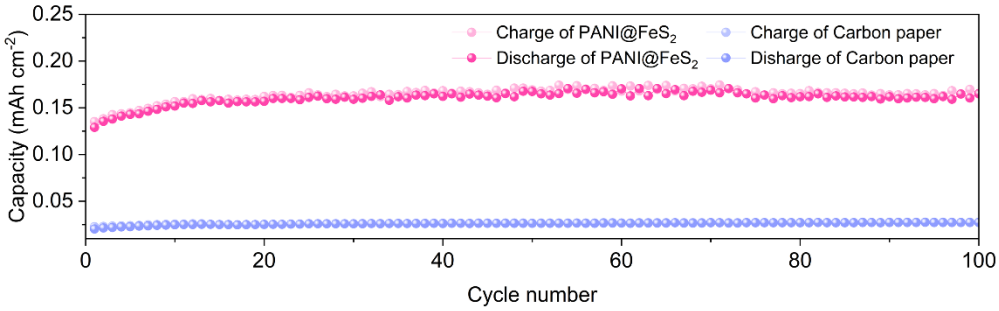

Fig. S10. Cycling performance of the PANI@FeS_2 hybrid and carbon paper at 1.0 mA cm^{-2}.

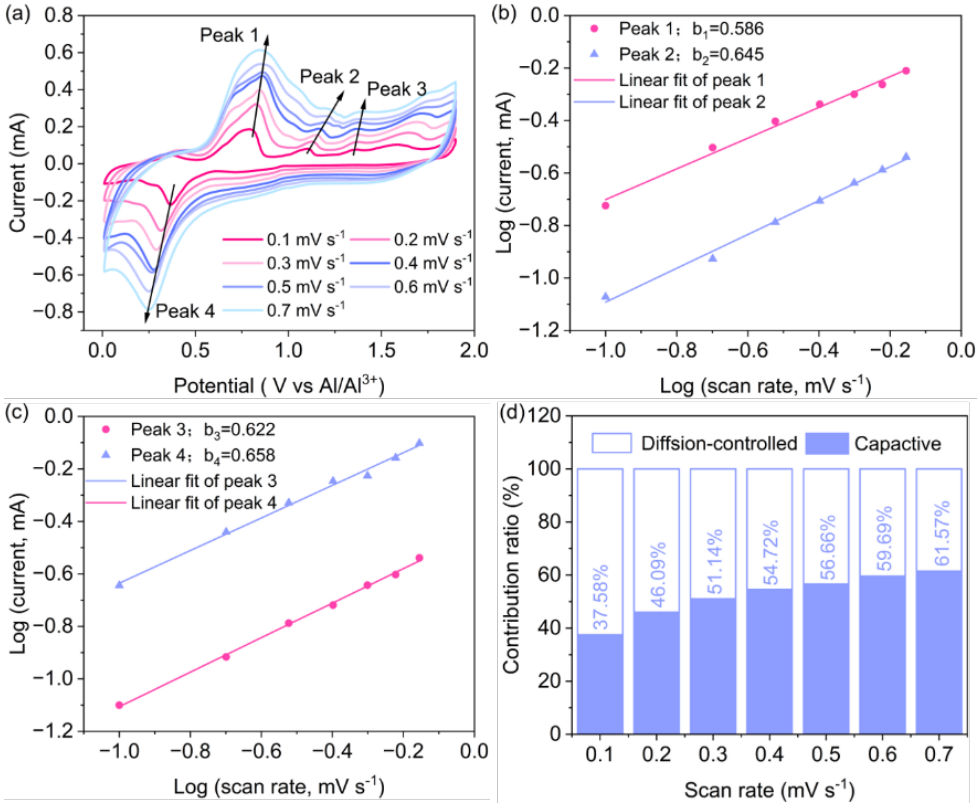

Fig. S11. (a) CV curves of pure FeS_2 cathode with scanning rates from 0.1 to 0.7 mV s^{-1}. (b, c) the log(*i*) *vs.* log(*v*) of oxidization and reduction peaks. (d) Contribution ratio of capacitive and diffusion-control processes.

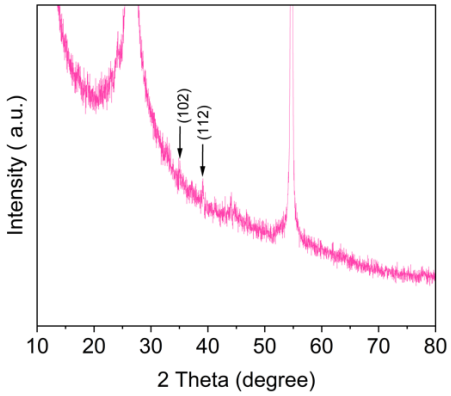

Fig. S12. XRD pattern of the PANI@FeS_2 hybrid after 100 cycles at 1.0 A g^{-1}.

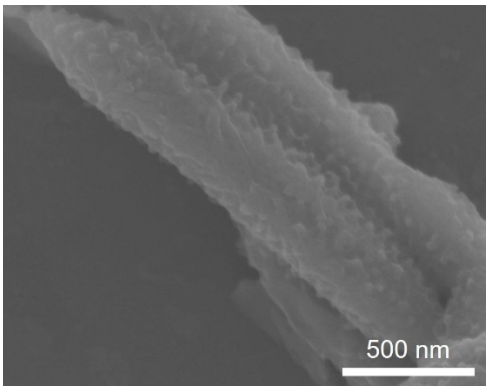

Fig. S13. SEM morphology of the PANI@FeS_2 hybrid after discharge at 1.5 A g^{-1}.

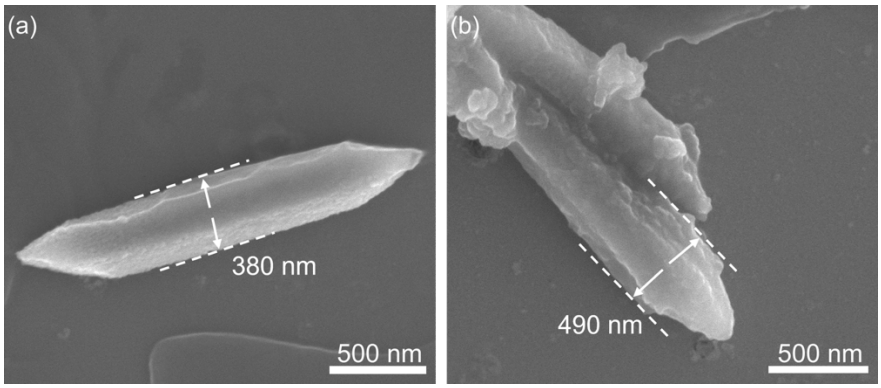

Fig. S14. SEM morphologies of FeS_2 (a) before and (b) after Al^{3+} ion insertion at 1.5 A g^{-1}.

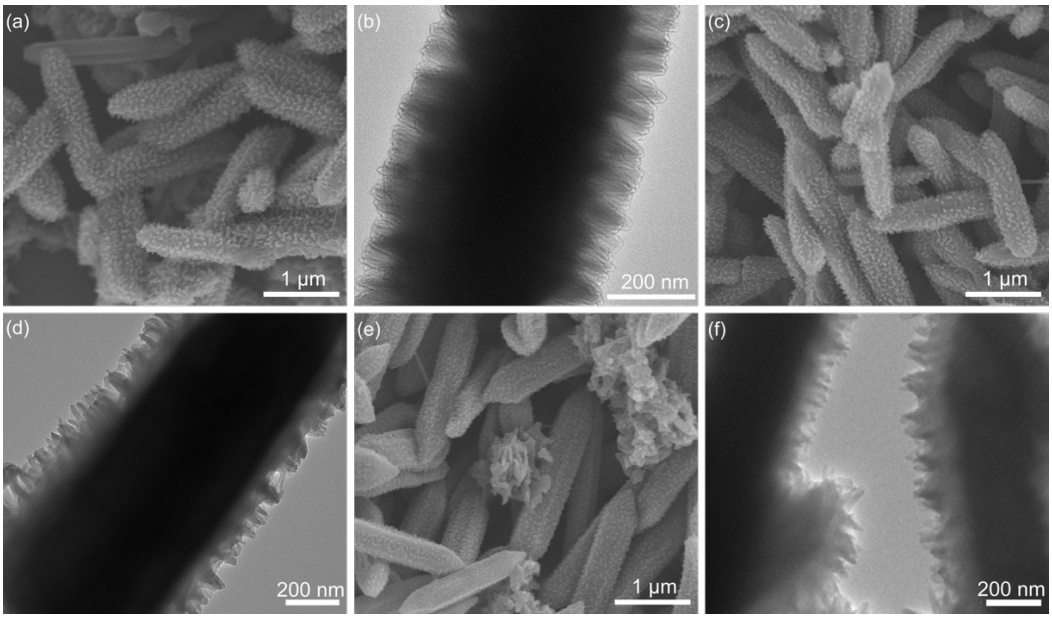

Fig. S15. SEM and TEM images of PANI@FeS_2 hybrid prepared by using (a, b) 0.284, (c, d) 0.355 and (e, f) 0.426 mL of aniline.

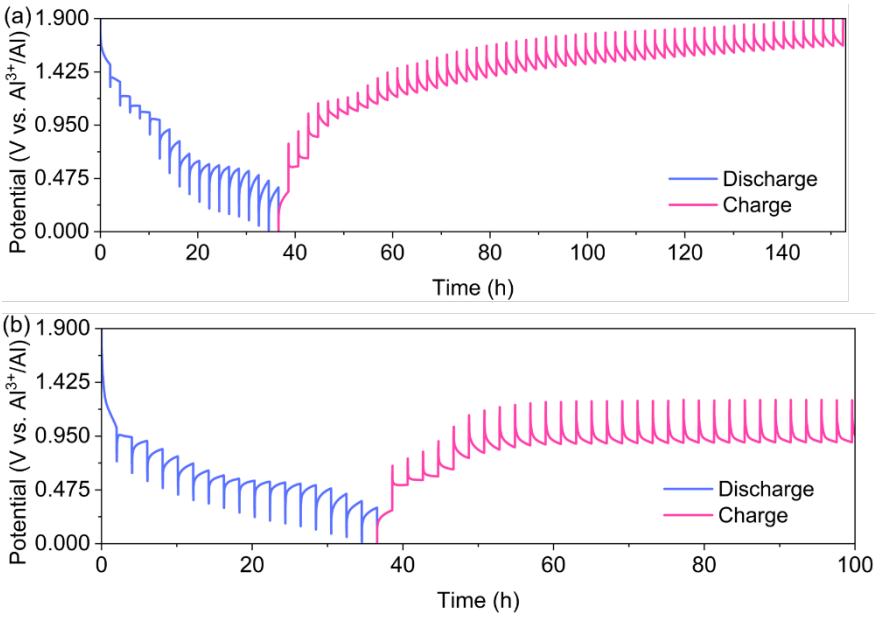

Fig. S16. GITT time–potential distributions of (a) the PANI@FeS_2 hybrid and (b) FeS_2 microrods.

Table S1. Comparison of battery performance with various cathode materials.

Materials	Current density (A g^{-1})	Cycle number	Capacity (mAh g^{-1})	Ref.
Ni_2CoS_4 nanosheets	0.1	100	143.8	1
TiO_2 nanorods	0.5	150	91	2
Co_3O_4@MWCNTs polyhedrons	0.1	150	125	3
MoO_2@Ni	0.1	100	90	4
Mo_6S_8 nano-blocks	0.04	100	66.7	5
VS_2 nanosheets	0.1	50	59.4	6
G-VS_2 nanosheets	0.1	50	88.3	6
V_2CT_x nanosheets	0.1	100	90	7
CoS_2@CNTs	0.1	100	60	8
SnSe nanoparticles	0.3	100	107	9
$Cu_{2-x}Se$ nanorods	0.2	100	100	10
Nanowire-on-nanorod PANI@FeS_2 hybrid	0.5	100	238.7	This work
	1	200	193.4	
	1.5	500	152.8	

References

1 S. Li, J. Tu, G. Zhang, M. Wang and S. Jiao, *J. Electrochem. Soc.*, 2018, **165**, A3504-A3509.

2 S. Wang, K. V. Kravchyk, S. Pigeot-Remy, W. Tang, F. Krumeich, M. Wörle, M. I. Bodnarchuk, S. Cassaignon, O. Durupthy, S. Zhao, C. Sanchez and M. V. Kovalenko,

ACS Appl. Nano Mater., 2019, **2**, 6428-6435.

3 X. Xiao, M. Wang, J. Tu, Y. Luo and S. Jiao, *ACS Sustain. Chem. Eng.*, 2019, **7**, 16200-16208.

4 J. Wei, W. Chen, D. Chen and K. Yang, *J. Electrochem. Soc.*, 2017, **164**, A2304-A2309.

5 L. Geng, G. Lv, X. Xing and J. Guo, *Chem. Mater.*, 2015, **27**, 4926-4929.

6 L. Wu, R. Sun, F. Xiong, C. Pei, K. Han, C. Peng, Y. Fan, W. Yang, Q. An and L. Mai, *Phys. Chem. Chem. Phys.*, 2018, **20**, 22563-22568.

7 A. VahidMohammadi, A. Hadjikhani, S. Shahbazmohamadi and M. Beidaghi, *ACS Nano*, 2017, **11**, 11135-11144.

8 K. Zhang, T. H. Lee, J. Cha, H. Jang, M. Shokouhimehr and J. W. Choi, *Electron. Mater. Lett.*, 2019, **15**, 727-732.

9 Y. Zhang, B. Zhang, J. Li, J. Liu, X. Huo and F. Kang, *Chem. Eng. J.*, 2021, **403**, 126377.

10 J. Jiang, H. Li, T. Fu, B. Hwang, X. Li and J. Zhao, *ACS Appl. Mater. Interfaces*, 2018, **10**, 17942-17949.